Severely Corroded RC with Cover Cracking

SEVERELY CORRODED REINFORCED CONCRETE WITH COVER CRACKING

Dario Coronelli [1], Kamyab Zandi Hanjari [2], Karin Lundgren [3]

[1] Assistant Professor
Contact author:
dario.coronelli@polimi.it
Politecnico di Milano, Dipartimento di Ingegneria Strutturale,
Piazza Leonardo da Vinci 32, 20133 Milano, Italy
Tel.+39-02-2399-4395 Fax +39-02-2399-4220

[2] PhD, Chalmers University of Technology, Department of Civil and Environmental Engineering, Gothenburg, Sweden

[3] Associate Professor, Chalmers University of Technology, Department of Civil and Environmental Engineering, Gothenburg, Sweden

Abstract. It is not uncommon that cover cracking, spalling and delamination have occurred. Previous research has mainly been concerned with corrosion levels leading to cover cracking along the main reinforcement, while corrosion of stirrups is often overlooked. Corrosion phenomena including stirrup corrosion were studied in an experimental investigation presented in this paper. High levels of corrosion were reached, up to 20% of the main bars and 34% of the stirrups legs. The occurrence of crack initiation, propagation and cover delamination were examined. The specimens had the shape of a beam end and were corroded with an accelerated method; an imposed current was used, taking care to keep the current density as low as practically possible for the duration of the laboratory testing. The effects of this process are compared with those of natural corrosion using models from the literature. The location of the bar, middle and corner placement, the amount of transverse reinforcement and the corrosion level of longitudinal reinforcement and of transverse reinforcement were studied. The results concerning the concrete cracking in the experimental campaign are presented here. The crack patterns and widths are analysed, showing differences between specimens with or without stirrups and when stirrups are corroding or not. Finally, the effect of corrosion was simulated as the expansion of corrosion products in a finite element model, and the results, mainly the crack pattern and width, are compared with the test results. The conclusions address the importance of taking into consideration both high corrosion levels and corrosion of stirrups for the assessment of deteriorated structures.

KEYWORDS: Concrete structures; Corrosion; Cracking; Anchorages; Beams; Finite Elements.

INTRODUCTION

Corrosion of steel reinforcement is one of the most common causes of deterioration of reinforced concrete, caused by either chloride penetration or carbonation of the concrete. Study of concrete cracking due to corrosion is necessary to assess the durability of a structure over time (Mullard and Stewart, 2011), taking into consideration both serviceability and strength (Val et al., 2009). In the presence of high levels of corrosion it is not uncommon that cover spalling and delamination occur (Fig.1). The consequent reduction of bond strength, together with the damage of the concrete and the steel cross-section loss, can well be a major problem in the performance of structures (Zandi Hanjari et al. (2011-a); Coronelli and Gambarova, 2004).

Previous research on corrosion cracking and bond of corroded reinforcement (Fib, 2000) has mainly been concerned with the corrosion of the main reinforcement of specimens without transverse steel, rarely comparing the behaviour of tests with and without stirrups (Alonso et al., 1998). To the knowledge of the authors, no study exists in which bond test specimens with corrosion of both main bars and stirrups have been investigated. Field investigations and tests on beams (Higgins and Farrow, 2006) have shown that cover delamination is more probable in areas with stirrups, even more if these are tightly spaced. The effect of corroded stirrups on crack initiation, crack propagation and cover delamination, in relation to the study of bond and of the overall structural performance therefore needs to be investigated more closely.

A research program comprising both the study of corrosion cracking and bond strength deterioration has thus been set up. Concrete cracking is studied here. The effect of this type of damage on the bond strength of RC specimens is presented by Zandi Hanjari et al. (2011-b). Specimens with and without stirrups were cast; for the former, in some of the specimens, the stirrups were protected from the corrosion process, whereas the others had both main steel and stirrup corrosion.

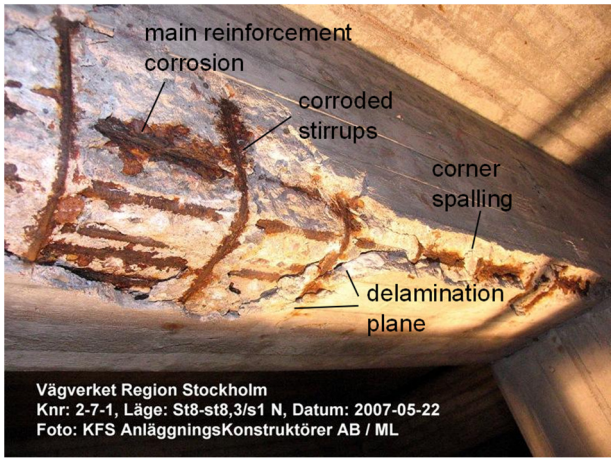

Fig.1 Delamination and corrosion of main bars and stirrups (photograph courtesy of Magnus Lindqvist)

The study obtained corrosion by imposed current, with maximum levels of cross-section loss reaching up to around 20% of the main reinforcement cross-section and 34% for the stirrups. Accelerated corrosion tests are widely used in the laboratory to study the mechanical properties of deteriorated RC specimens. The chemo-physical effects are different from those of natural corrosion (Alonso et al., 1998). From a mechanical point of view, some concerns exist regarding spurious bond deterioration obtained with high current densities (Yuan et al., 2007; Sæther, 2009). The choice of high values of current density ranging from 20 to 100 A/m^2 has been made in the literature to save time with short duration corrosion tests (Al-Sulaimani et al., 1990; Almusallam et al., 1997). Clark and Saifullah (1993) tested specimens corroded with current densities from 0.5 to 20 A/m^2, showing that spurious bond deterioration started for values higher than 5 A/m^2. For this reason the study presented here used a reasonable current density, on average around 1 A/m^2 (=100 μA/cm^2); the maximum corrosion levels were reached after nearly one year.

Vidal et al. (2004) corroded beams naturally for a time up to 17 years. On the basis of the test results for cracking and corrosion penetration, these authors proposed a model relating crack width to the corresponding reinforcement weight loss. Their natural corrosion results are compared with the artificial corrosion results in this paper. To this aim a recent study by Mullard and Stewart (2011) is used. These Authors compared the different crack growth rates measured with low and high corrosion rates, proposing a correction factor to obtain predictions of crack opening in time for the very slow natural corrosion processes, starting from the data obtained in the much faster artificial corrosion processes.

Furthermore, the effect of corrosion on the reinforcement, on the surrounding concrete and on their interaction can be simulated through three-dimensional non-linear finite element analysis. A review of existing models for corrosion-induced crack initiation and propagation has been presented by Val et al. (2009). Although detailed structural analyses are numerically expensive, they allow for a more accurate description of the corrosion damage at the material and structural levels. Volume expansion of corrosion products, that leads to cover cracking and spalling, significantly influences the confinement conditions and consequently the steel/concrete bond. These effects have been taken into account in bond and corrosion models previously developed by Lundgren (2005a, 2005b). In the present work, numerical analysis was used to better understand the effects of corroding stirrups on the crack patterns and crack width.

The model proposed by Berra et al. (2003), which is an extension of the model by Molina et al. (1993), accounts for the effect of rust flow through cracks using a correction factor. Val et al. (2009) have also studied the phenomenon of corrosion products penetrating into concrete pores and cracks throughout investigation of the thickness of the porous zone and the extent of corrosion products that penetrate into cracks. A final discussion is added regarding the prediction of crack widths in relation to the corrosion level reached by the model in this paper. The problem of corrosion products flow in the cracks is further studied in Zandi Hanjari et al. (2011-c).

In the following, the specimens and the corrosion setup are described. Results on the concrete cracking, crack patterns and reinforcement corrosion are presented. The progressive crack opening and propagation was observed over a period of eleven months. Increasing crack width measurements were made for the lower corrosion levels. Final crack values at high corrosion levels are reported. Comparisons of different crack patterns and their evolution are made in the different types of specimens. The corrosion level was calculated from the circulated current and

measured by the gravimetric method after the tests. Finally, the effect of corrosion was simulated as the expansion of corrosion products in a finite element model, and the results, mainly the crack pattern and width, are compared with the test results. The conclusions point out the differences in tests with and without stirrups, and the significant effects of stirrup corrosion.

EXPERIMENTAL SET-UP

Specimen geometry and materials

The specimens had the shape of a beam end after inclined shear cracking (Fig.2a). The concrete specimens (Fig.2b) were reinforced with longitudinal bars with 20 mm diameter and stirrups with 8 mm diameter. The main bars were in contact with the concrete over a length of 210 mm. A concrete cover of 30 mm to the main bar was used. The concrete was an ordinary type with an average cubic strength of 37.5 MPa without chlorides for the control specimens and 34.3 MPa with 3% chlorides in the mix of the specimens with corrosion.

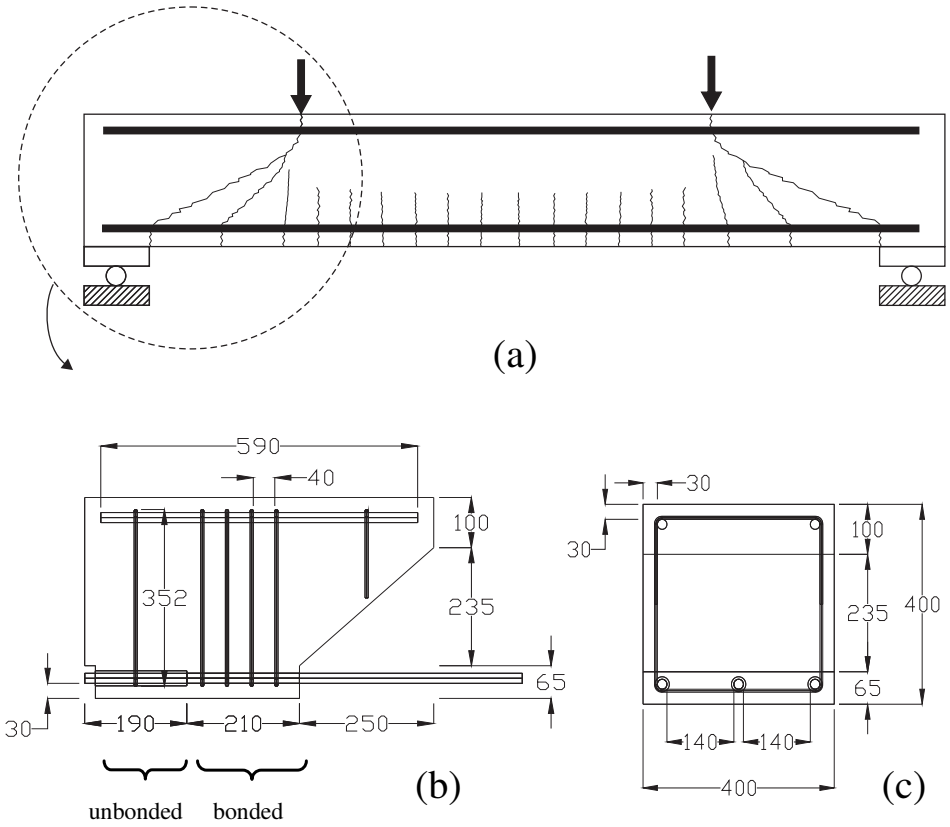

Fig.2 **Test specimens: (a) schematic illustration of a beam end; (b-c) geometry and reinforcement for specimens types B and C; in type A the stirrups in the bonded length were removed. All dimensions are in mm.**

The influences of the bar location, middle and corner placement, the presence or absence of transverse reinforcement, the corrosion level of longitudinal reinforcement and corrosion of transverse reinforcement were studied. The specimens were of three different types (Table 1) in relation to the reinforcement arrangement and corrosion: specimens without stirrups and only main bar corrosion (Type A); main bars corroding while the stirrups were protected by insulating tape (Type B); and main bars and stirrups corroding (Type C). After corrosion, bond tests were carried out; these are described in Zandi Hanjari et al. (2011-b).

In the marks in Table 2, the first letter indicates the specimen type (A, B or C), the second number the corrosion level at which corrosion was stopped (1, 2 or 3) the third letter indicates the position of the bar for the bond test (corner or middle); the final number distinguished specimens for otherwise identical couples for middle bar bond tests.

Artificial corrosion

The specimens were corroded with an electrochemical method, using impressed current (Fig.3). The current flowed through the main bars across the concrete cover to a cathode placed at the top of the beam, inside a tank containing a solution of 3% chlorides.

The stirrups in Type B specimens were isolated using tape, to avoid corrosion. The stirrups in Type C were not isolated; thus they were in contact with the main bars. In these specimens, 45% of the surface through which the current flowed was made up of the stirrups and 55% of the main bars; these values were used to calculate the current that circulated in each type of reinforcement, and the corrosion level, as will be described in the following.

The current density average value up to Level 1 was 0.5 A/m^2 for specimens with and without stirrup corrosion. Beyond Level 1, the current density was increased to an average value of 1.52 A/m^2 for both specimens, i.e. with and without stirrup corrosion. The average current density in time over the whole corrosion duration was $i_{corr,exp}$ = 1.16 A/m^2. Among artificial corrosion tests in the literature, these can be considered reasonable values. Other researchers have used faster rates, by even one order of magnitude, as already mentioned in the Introduction.

Table 1 Test program

Specimens and corrosion levels	Number of specimens		
	Without stirrups [(1)] (Type A)	With non-corroded stirrups [(1)] (Type B)	With corroded stirrups [(1)] (Type C)
Reference - 0% weight loss	5	6	-
Level 1 - Cracks along the main reinforcement; approximately 1% weight loss (average value)	-	2	-
Level 2 - Propagation of cracks; approximately 10% weight loss (average value)	2	1	1
Level 3 - High Corrosion; approximately 15% weight loss (average value)	-	4	2

[(1)] Along the embedment length

Table 2 Corrosion levels – Main bars

Level	Specimen (^)	Weight loss (%)	Average penetration (mm)	Position (°)
1	B1(c)	0.2	0.01	right
		1.4	0.07	central
		3.5	0.18	left
	B1(m2)	2.1	0.10	right
		0.7	0.04	central
		0.2	0.01	left
2	A2(c)	8.9	0.46	right
		8.5	0.43	central
		7.3	0.37	left
	A2(m)	9.0	0.46	Right
		4.5	0.23	Central
		7.2	0.37	Left
	B2(m1)	7.7	0.39	Right
		4.2	0.21	Central
		12.4	0.64	Left
	C2(m2)	15.5 (*)	0.81	Right
		7.0 (*)	0.35	Central
		9.8 (*)	0.50	Left
3	B3(c)	12.9 (*)	0.56	Right
		11.6 (*)	0.59	Central
		10.9 (*)	0.66	Left
	B3(m1)	13.5	0.61	Right
		14.8	0.59	Central
		13.0	0.74	Left
	B3(m2)	9.2	0.47	Right
		14.0	0.75	Central
		15.7	0.82	Left
	C3(c)	7.0	0.57	Right
		16.7	0.87	Central
		11.1	0.36	Left
	C3(m1)	21.0 (*)	1.10	Right
		19.1 (*)	1.01	Central
		20.7 (*)	1.11	Left

(^) Mark: Specimen type (A, B, C) – Final Corrosion level (1, 2, 3) – Bar to be loaded in bond tests (c = corner; m = middle) – Specimen nr. (1, 2).
(*) Calculated from the circulated current.

Table 3 – Corrosion levels - Stirrups

Specimen	weight loss (%)	penetration (mm)	Level	position (*)	notes
C2(m2)	12	0.25	2	-	calculated
C3(m1)	23	0.48	3	-	calculated
C3(c)	13	0.27	3	Front	measured
	24	0.51		Central	
	27	0.57		Central	
	34	0.75		Back	

(*) Front and back relative to loaded end of bar in scheme

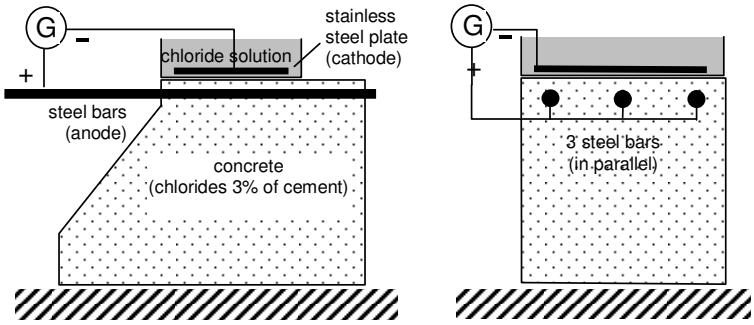

Fig.3 Accelerated corrosion set-up.

The current flowing in each reinforcement bar was measured at intervals, and the corrosion level reached was calculated using Faraday's law. After the bond tests, the specimens were broken up to extract the bars, and the maximum corrosion levels were measured by the weight loss measurements with the gravimetric method of the ISO 8407 standard. The oxide layer at the interface between the remaining virgin steel bar and the concrete undergoes mechanical damage in the bond test, but the quantity and weight of the underlying virgin steel are not affected. The gravimetric loss is obtained as a difference between the initial bar weight and that of the remaining virgin steel. Hence there is no effect of the mechanical damage of the bond test on the weight loss. The values in the gravimetric measurements were approximately 10% less than the values calculated by Faraday's law. The difference between measurements carried out with the two methods is related to the bar being embedded in concrete: an amount of energy is needed to initiate the corrosion, and the concrete permeability influences the evolution of the process (Auyeung et al., 2000). The corrosion levels for one specimen of Type A and two specimens of Type C were calculated only from the circulated current, because these specimens will be subjected to mechanical testing later on and thus have not yet been broken up. The effective corrosion of the reinforcement in these three specimens can be estimated on average as 90% of the value calculated using Faraday's law.

The corrosion was planned according to three different levels of penetration (on average):

- *Level 1,* corresponding to cracks propagating along the main reinforcement for a corrosion level around 1% weight loss;
- *Level 2,* corresponding to approximately 10% corrosion;
- *Level 3,* aiming to reach delamination for high corrosion levels, around 15% weight loss.

The specimens were corroded for periods from three to eleven months. The average corrosion levels reached for Level 1, 2 and 3 were 1.3%, 7.1%, and 13.8%, respectively.

Crack widths on the top and side cover were measured during the corrosion process using a microscope with a resolution of 0.04 mm up to corrosion Level 1. Beyond this level, most cracks were filled by corrosion products to a point that the optic device could no longer be used. Crack widths at Levels 2 and 3 were measured before the mechanical testing by using a reference ruler with a range of graded lines, each corresponding to a specified width.

The corrosion in the main reinforcement affected about half of the main bars, i.e. the surface facing the outer concrete cover. For the transverse reinforcement, the deterioration regarded the portions of the stirrup parallel to the bottom cover in Fig.2, the corner bends and a short length of a few centimetres parallel the sides of the beam, close to the bottom cover. In these parts of the stirrup, the whole surface all around the perimeter was affected. Corrosion was spread over these surfaces, with some pitted zones. However, note that the average corrosion values in Table 2 were calculated from the weight loss, assuming a uniform depth of the corrosion on the whole bar surface.

RESULTS

Corrosion Level 1

Between corrosion initiation and Level 1, all specimens showed longitudinal cracks along the main bars. The corrosion level at first cracking was about 30-50 microns average penetration (0.6-1.0% weight loss), with little difference in the three types of specimens. The first cracks opened on the top cover; here, measurements were made at intervals at all corrosion levels. The corrosion level at each measurement time was calculated from the circulated current, obtaining diagrams such as those shown in Fig.4.

In Type C specimens, up to the first level of corrosion planned, the main bars corroded more slowly because of the current taken by the stirrup corrosion. The corrosion level reached at this stage and the crack widths were hence smaller. To reach Levels 2 and 3 for this type of specimen, the current was increased to obtain a corrosion rate for the main bars close to that of the other specimens.

In addition to the cracks in the top cover, Specimen A2c showed a crack on one side, and the initiation of a delamination crack visible on the front of the specimen. Some cracks visible on the front also formed for B3c and C3c. The crack patterns are further analysed in the following.

Corrosion Level 2

Moving from Level 1 to Level 2, parts of the cracks visible on the front of some of the specimens joined to form delamination cracks connecting two or three main bars (Fig.5). The measurements of the top cover cracks with a microscope were suspended because the accumulation of corrosion products made these observations inaccurate. Typical crack patterns are depicted for one specimen of each type in Fig.5, together with the corresponding crack widths in the tables.

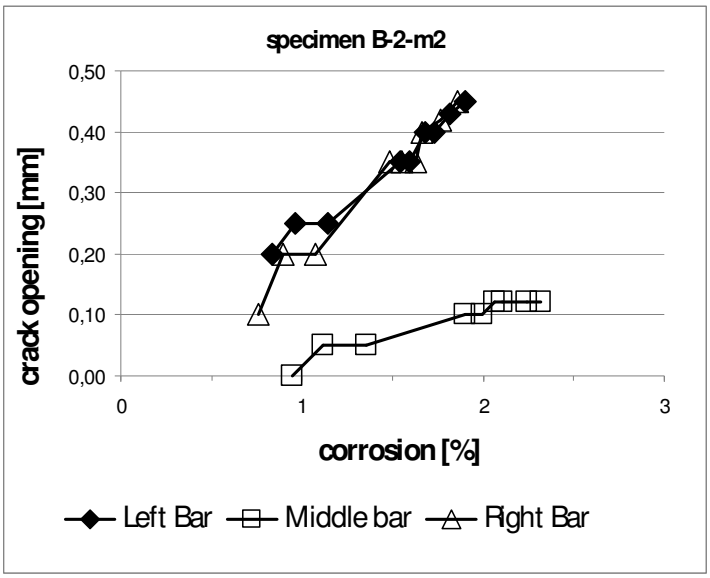

Fig.4 Level 1, top cover crack width measurements.

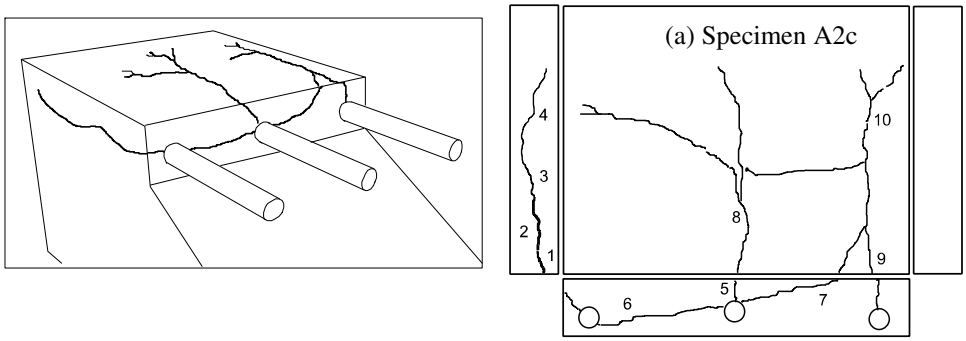

Crack nr.	1	2	3	4	5	6	7	8	9	10
Width (mm)	1.4	1.0	1.0	0.9	0.5	0.5	0.2	0.4	0.6	0.4

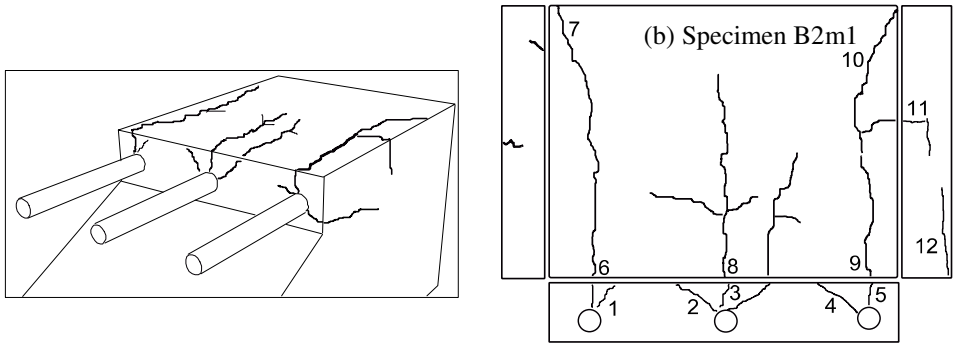

Crack nr.	1	2	3	4	5	6	7	8	9	10	11	12
Width (mm)	0.50	0.30	0.35	0.20	0.4	0.5	0.9	0.4	0.4	0.3	0.4	0.2

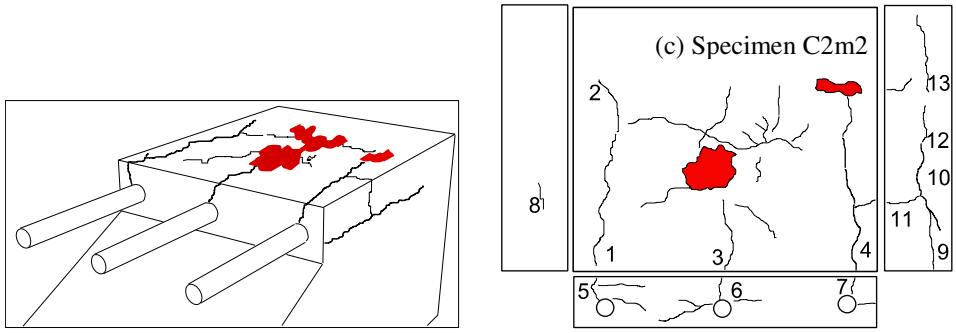

Crack nr.	1	2	3	4	5	6	7	8	9	10	11	12	13
Width (mm)	0.4	0.2	0.1	0.3	0.2	0.15	0.15	0.05	0.1	0.3	0.25	0.25	0.1

Fig.5 Level 2 crack patterns and widths.

Specimens without stirrups (Type A): the cracks run mainly along the longitudinal reinforcement. These specimens showed fewer and wider cracks than those with stirrups. In one specimen (A2c) a delamination plane formed, with a maximum crack width of 1.4mm (Fig.5-a).

Specimens with noncorroded stirrups (Type B): longitudinal cracks opened in the top and side covers (Fig.5b). The crack pattern on the front cover had different features according to the specimen: either cracks radiating from the main bars to the closest point of the outer surface;

cracks lying in a horizontal plane; cracks in inclined planes forming a V-shaped pattern. Longitudinal and transverse cracks formed on the side covers.

Specimens with corroded stirrups (Type C): the presence of corroding stirrups caused a more complex crack pattern than for the other types of specimens. Type C specimens showed different types of cracking and damage in addition to the longitudinal cracks, opened at level 1 (Fig.5c):

- A top cover cracking with many small cracks opened, both longitudinally and in other directions;
- Initiation of delamination cracks, forming a plane connecting the bars; these could be observed on the front and on the side covers, in a plane parallel to the main reinforcement;
- Side cover cracks in transverse directions, with respect to the bar axis;
- Corrosion products in big stains on the outer surface of the top cover.

Corrosion Level 3

The corrosion process was continued to a level of around 15% weight loss. The widening of the longitudinal cracks on the top cover slowed down. This can be interpreted by considering the flow of the corrosion products within cracks propagated in the horizontal plane, with a smaller pressure build-up with respect to the cracks radiating around the bar across the smaller cover. This will be further discussed in relation to the crack width *vs.* corrosion level plots shown later in this paper.

Crack patterns and maximum crack width values are shown in Fig.6 for three of the four specimens reaching level 3; specimen B3m2 (not shown in Fig.6) had cracks very similar to B3C. No specimen of Type A without stirrups was corroded up to this level.

The typical crack pattern is shown in Figure 6a for Type B specimens, with two curved splitting cracks, at an opposite curvature, connecting the middle and one of the corner bars. Similar cracks are known to occur in the double notch edge fracture test (Grassl and Rempling, 2006) where normal and shearing stresses act together, producing curved crack patterns.

For Type C specimens, the cracks initiated at Level 2 developed into delamination cracks, visible on the outer surface both on the front of the specimen and on the lateral covers. The examination of the corrosion cracks breaking up specimen C3c with corroded stirrups after the load tests (Fig.7) highlights the presence of a delamination plane, running across the corroding stirrups and isolating the portion of concrete covering the stirrups. Fig.7 shows that these cracks connected with those originating from the main reinforcement, with a lot of rust accumulation highlighted by the rust stains and the oxides penetrating into the pores of the concrete.

The cracks over the corroding stirrups on the top cover were very small. The maximum width for this last type of cracks shown in Figs.5c and 6b-c was around 0,1mm. The cracks were visible up to level 2; rust accumulation at level 3 made the visual observation of these thin cracks difficult.

On the whole a rather smeared damage was observed. The morphology could be partly different with more widely spaced stirrups: in this case cracks opening along the lines of the transverse reinforcement are frequently observed in corroding beams (Higgins and Farrow, 2006). Future

research could study the different crack patterns obtained varying the spacing of the transverse stirrups, and the cover to bar diameter ratio for this type of reinforcement.

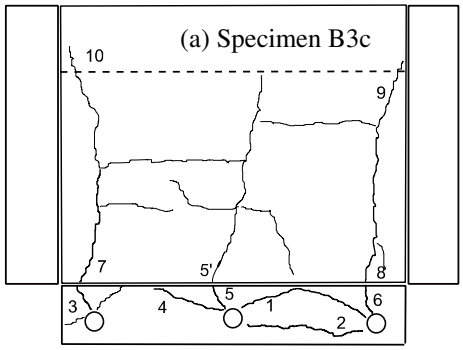

Crack nr.	1	2	3	4	5	5'	6	7	8	9	10
Width (mm)	0.40	0.20	0.50	0.3	0.2	0.1	0.5	0.4	0.35	0.3	0.2

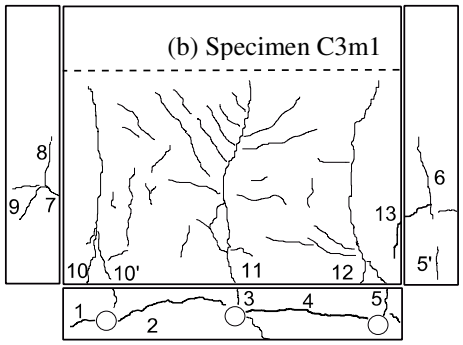

Crack nr.	1	2	3	4	5	5'	6
Width (mm)	0.3	0.3	0.35	0.40	0.25	0.2	0.15
Crack nr.	7	8	9	10	11	12	13
Width (mm)	0.35	0.15	0.3	0.15	0.1	0.1	0.35

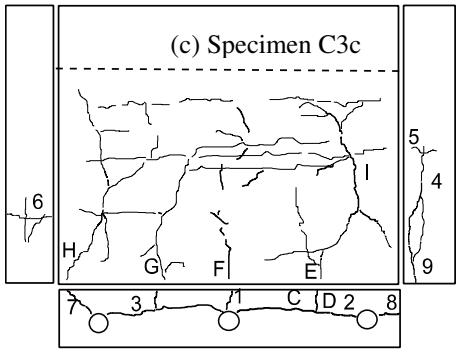

Crack nr.	1	2	3	4	5	6	7	8
Width (mm)	0.30	0.30	0.30	0.35	0.20	0.15	0.30	0.45
Crack nr.	9	C	D	E	F	G	H	I
Width (mm)	0.35	0.45	0.20	0.25	0.20	0.15	0.20	0.30

Fig.6 Level 3 crack patterns and widths.

Fig.7 Delamination plane formed by corrosion cracks running across stirrups, specimen C3c: cover removed after the bond test on the specimen.

Comparison with results in the literature

To compare the artificial corrosion results in this paper with slow natural corrosion results a procedure by Mullard and Stewart (2011) is used. Studying the opening of cracks with corrosion increasing in time, the Authors showed the dependence of the crack growth on the corrosion rate. The effects of a low corrosion rate $i_{corr,\ real}$, simulating the real natural conditions in an interval of time $t_{cr,real}$ are compared to those of a high corrosion rate $i_{corr,\ exp}$, imposed experimentally in an interval of time $t_{cr,exp}$. For a given crack width, in a slow process the corrosion penetration $p_{corr,real}$ is less than the penetration $p_{corr,exp}$ in an artificial process. These Authors determined experimentally the values of the rate of loading factor:

$$k_r = (t_{cr,\ real}\ i_{corr,\ real}) / (t_{cr,\ exp}\ \ i_{corr,\ exp}) = \ p_{corr,real} / p_{corr,exp} \qquad (0.25<k_r<1) \quad (2)$$

where $p_{corr} = 0.0116\ i_{corr}\ t$, from Faraday's law (Alonso et al. ,1998). For the artificial corrosion tests shown here, the corrosion rate is approximately 20 to 100 times higher of that in natural conditions, corresponding to $k_r = 0.25$. The results of this are shown in Fig.8, where the corrosion levels of the tests are obtained from the penetration multiplied by k_r.

Fig.8 also shows the model by Vidal et al. (2004), obtained from crack width measurements along the main bars of beams corroded in a saline environment and subjected to wetting–drying cycles over periods of 14 and 17 years. The corrosion rate and the oxides produced were close to those actually observed in natural conditions. On the basis of the tests Vidal et al. proposed an empirical linear expression predicting crack propagation for the main bars:

$$w = K\ (\Delta A_s - \Delta A_{so}) \qquad (1)$$

where: w = equivalent crack width (mm); ΔA_s = the steel loss of cross section (mm^2); ΔA_{so} = the steel loss of cross section at the initiation of cracking, (mm^2); $K = 0.0575$.

The crack width measurements were related to the corresponding reduction of cross section ΔA_s by measuring the weight loss. Local weight loss measurements were made by weighing the bar before casting the beams and short portions cut from the bar after corrosion. An equivalent crack width w was obtained as the sum of crack widths corresponding to the same corroded portion of one bar.

Fig.8 also shows the results in this experimental program for the main bars (divided in three groups, type A, B and C specimens). The corrosion is the average weight loss of the bar; this is a reasonable approximation for the corrosion of the bars in the tests, that was rather uniformly distributed, as generally seen in artificial corrosion tests. As already mentioned, the corrosion levels in Fig.8 for these tests are modified using Equation 2. The equivalent crack width is calculated as the sum of crack widths measured on the front cover (i.e. on the plane perpendicular to the main bars). This position was chosen because the presence of several cracks departing from the same main bar can be observed there, including the delamination cracks connecting the middle and corner bar.

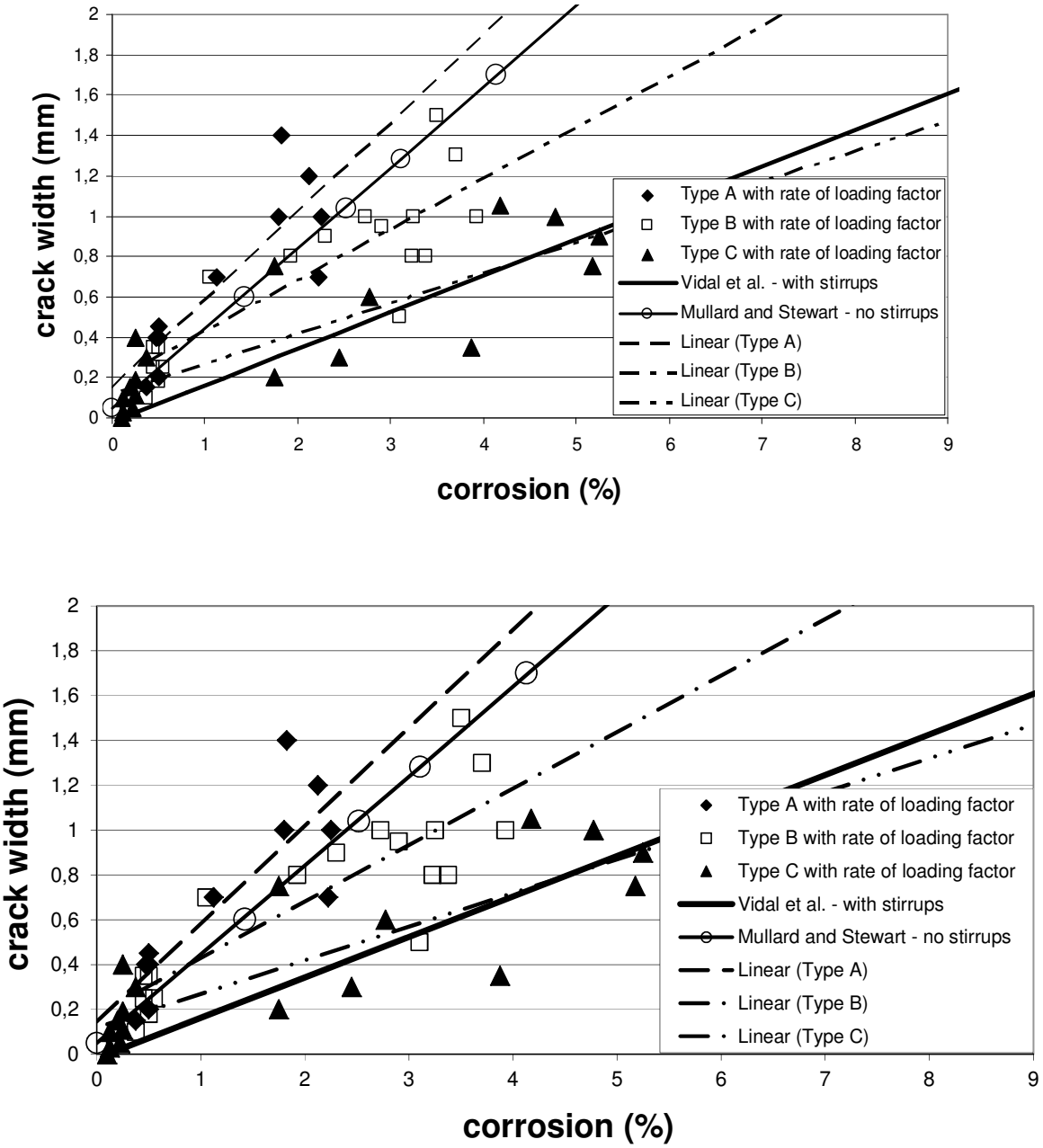

Fig.8 Comparison of test results, considering rate of loading correction factor, with natural corrosion results by Vidal et al. (2004) and model by Mullard and Stewart (2011).

The results for specimens without stirrups (Type A) show wider crack openings compared to the specimens with transverse steel. The crack widths for Type B and C specimens are lower, as also shown by the linear fit lines. This can be interpreted as the effect of the stirrup confinement. The smaller crack widths in specimens with corroding stirrups (Type C) can be explained as a result of a more spread damage of the cover, as will be further shown in the next section.

It is remarkable that the results obtained for the type C specimens in this study agree quite closely to the results of equation (1) by Vidal et al. (2004) for natural corrosion. The Vidal et al. (2004) model is based on tests with a range of cover/diameter ratios (c/d=1.33-3); in this study the c/d ratio was 1.5, which is within this range. The concrete strength was similar (45 vs 37.5 MPa cubic strength). The stirrups were 6mm or 8mm bars at 220mm for Vidal et al., while here 8mm at 40mm.

Moreover Mullard and Stewart (2011) proposed an analytical relation, based on tests without transverse reinforcement, to predict the crack width opening w in time for natural corrosion, here expressed as a function of corrosion penetration p_{corr}:

$$w = w_o + (r_{crack}/k_r)\,(p_{corr} - p_{corr,o})/(0.0116\, i_{corr,\,real})\, i_{corr,real}/(i_{corr,\,exp}\, 0{,}000114) \qquad (3)$$

where:

- r_{crack} = crack growth rate (mm/h), depending on the cover to bar diameter ratio c/d and the tensile strength of concrete f'_t ($r_{crack} = 0.0008\, e^{-1.7\,\Psi}$, $\Psi = c/(df'_t)$);
- p_{corr} , $p_{corr,o}$ = corrosion penetration (mm) for crack w and for first crack opening w_o;
- t, t_o = time (years) to reach crack width w, and first crack opening w_o;
- $(p_{corr} - p_{corr,o}) / (0.0116\, i_{corr,\,real}) = t - t_o$, from Faraday's law (Alonso et al. 1998; i_{corr} in $\mu A/cm^2$).

Results for Equation (3) are shown in Fig.8 with the parameters relative to the tests in this study: k_r =0.25, $i_{corr,exp}$ = 116 $\mu A/cm^2$, and $i_{corr,real}$ = 1$\mu A/cm^2$ (Mullard and Stewart, 2011). Corrosion in Fig.8 is calculated as percentual weight loss. Equation (3) was obtained from tests without transverse reinforcement. The results show a good correspondence to the tests for Type A specimens.

NUMERICAL MODELLING

The specimens were analysed in detailed 3D finite element (FE) models in the program DIANA (2009). The main purpose of the analyses presented here is that of studying the different crack patterns occurring in the different types of specimen. A final discussion is added regarding the prediction of crack widths in relation to the corrosion level reached by the model.

Because of symmetry, half of one specimen was modelled with a 10-mm element size. Four-node, three-side isoparametric solid pyramid elements were used for concrete, transverse and longitudinal reinforcement. A constitutive model based on non-linear fracture mechanics using a smeared rotating crack model based on total strain was applied for concrete (DIANA, 2009). The crack band width was assumed to be equal to the element size; this was later verified in the analyses. For the concrete in tension and compression, the models of Hordijk (1991) and Thorenfeldt (1997) were adopted, respectively. The reinforcing steel was modelled on the basis of an isotropic elasto-plastic model with the Von Mises criterion. The material properties in the analyses are given in Table 4.

Table 4 Material properties used in the analyses.

Mix	Concrete				Reinforcement		
	f_{cc}* [MPa]	f_{ct} [MPa]	G_F [N/m]	E_c [GPa]	f_y ^ [MPa]	E_c [GPa]	f_u ^ [MPa]
Reference specimens	29.7	2.33	64.3	29.42	510	200	610
Corroded specimens	27.7	2.19	61.2	28.74	510	200	610

* The values given are cylinder strength calculated from measured cubic strength.

^ The values given are the average of test results on a sample.

The bond and corrosion models used in the analyses have earlier been developed by Lundgren (2005a,b). The modelling approach is especially suited for detailed 3D FE analyses, where both concrete and reinforcement are modelled with solid elements. Surface interface elements are used at the steel/concrete interaction to describe a relation between the stress and the relative displacement in the interface. The interface elements include a bond model and a corrosion model, which can be viewed as two separate layers around a reinforcement bar. The bond model is a frictional model, using elasto-plastic theory to describe the relations between the stresses and the deformations. In the corrosion model, the effect of corrosion is simulated as the volume increase of the corrosion products compared to the virgin steel. The volume of the rust relative to the uncorroded steel, v_{rs}, and the corrosion penetration as a function of the time, p, is used to calculate the free increase of the bar radius, y, i.e. the increase in radius including the oxides when the normal stresses are zero:

$$y = -r + \sqrt{r^2 + (\nu_{rs} - 1)(2rp - p^2)} \qquad (4)$$

where r is the original bar radius. As the rust is not free to expand, the mechanical behaviour of the rust itself is included. The rust is assumed to have a mechanical behaviour similar to that of a granular material; that is, its stiffness increases with the stress level. The corrosion is then modelled by taking time steps. The corrosion model was shown to be capable of describing the effects of uniform and localized corrosion (Lundgren 2005b). Only the effect of uniform corrosion on half of the rebar cross-section was included in the numerical analysis of the test specimens.

The ratios of volumetric expansion of different typical oxides with respect to the virgin material, given in the literature (Liu and Weyers, 1998), vary between 1.7 for FeO and 6.15 for $Fe(OH)_3 3H_2O$, depending on the level of oxidation. For the volumetric expansion coefficient of rust the value of 2.0 suggested by Molina et al. (1993) is frequently used in numerical analyses of corroded concrete (Berra et al., 2003; Lundgren et al. 2007). Other studies proposed higher values: Val et al. (2009) used a value close to 3.0; Bhargava et al. (2006) proposed a value of 3.4 based on published experimental data. The value of 2.0 has been chosen in this study, on the basis of the numerical studies indicated above. The consequences of this choice are discussed in the following.

In a similar way as that in the experiments, the longitudinal bars were subjected to corrosion from the top cover, i.e. half of the cross-section was affected by corrosion; see Fig.9. The top leg of the stirrups was subjected to corrosion all around the cross-section. The vertical leg of

the stirrups was corroded down to the half of the longitudinal bar section. Unlike the experiments, the same corrosion penetration was imposed on all bars.

An incremental static analysis was made using a Newton-Raphson iterative scheme to solve the non-linear equilibrium equations. In a phased analysis, the corrosion was first applied. The external load was then applied on the bar. This paper presents only the study of the corrosion penetration and the related damage. For the bond tests see Zandi Hanjari et al. (2011-b).

Results

The crack patterns obtained are first shown and compared with the tests results. The crack widths for increasing corrosion levels up to the maximum reached are then compared with the test results. The maximum corrosion levels corresponded to extensive cover cracking; severe damage of concrete resulted in numerical instability in the analysis.

Globally, the crack patterns achieved in the numerical analyses agree well with the observation from experiments. Three main cover cracking patterns can be observed in the numerical analysis:

1. In the absence of stirrups (Type A, Figure 10a), the corrosion cracks around the corner bars propagate through the side and top covers, and a corner cover spalling takes place. This was also observed in the tests specimen A2m, while a delamination plane formed in A2c (Fig.5a).

2. In the Type B specimens (non-corroding stirrups, Figure 10b), the cracks initiated from the corner and middle bars formed a delamination plane. As already mentioned, the curved cracks correspond to those observed in double edge notched specimens (Grassl and Rempling, 2006). This was also observed in both tests specimens B3c (Figure 6a) and B3m2.

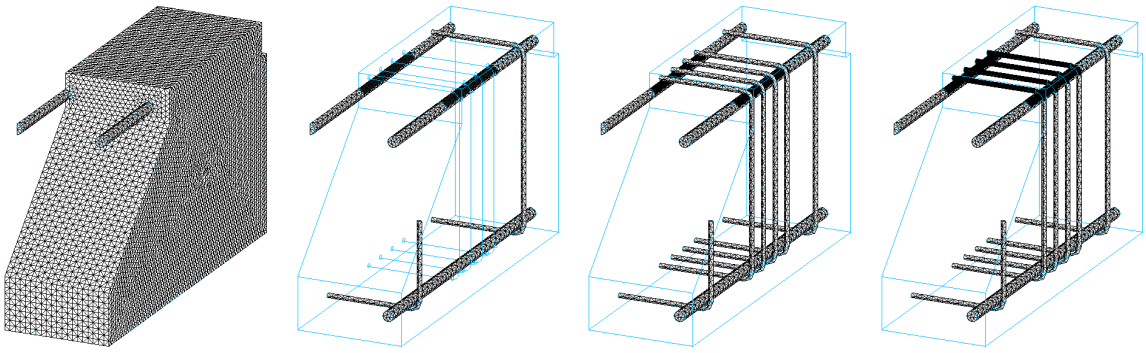

Fig.9 FE model of the specimens; the portions of the bars in dark grey were subjected to corrosion.

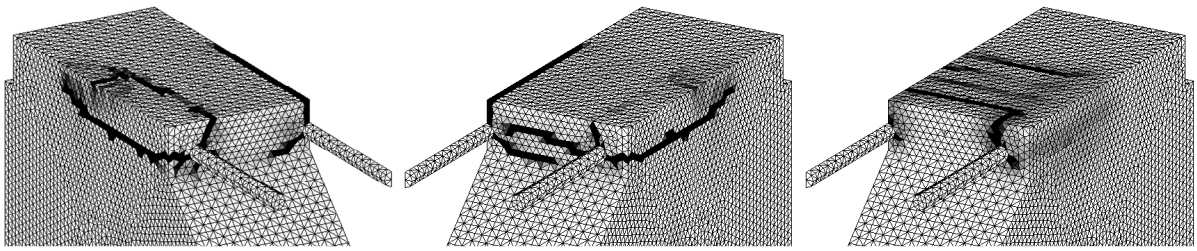

(a) (b) (c)

Fig.10 Numerical (half of the specimen) crack patterns: (a) Type A; (b) Type B; (c) Type C.

3. A different pattern was obtained when both longitudinal and transverse bars were corroded (specimens of Type C, Figure 10c). Cracks appeared transversely to the main bars, due to corroding stirrups before any of the former patterns occurred. Thus a more local cover crack pattern, mainly damage of the concrete between the stirrups, formed. The longitudinal cracks were also simulated, but with a smaller width than in the Types A and B. In addition, in the model a wide delamination crack runs between the central and corner bars, close to the level of the stirrups, without reaching the external surface of the specimen (Fig.11). This corresponds to the test results (Fig.7).

The crack widths on the top cover were evaluated from the numerical results for the nodal displacements on each side of the crack, and compared to the test results (Fig.12). The maximum crack width is underestimated for specimen A2c, is approximated correctly for B3c and is again underestimated for C3m1. The model correctly simulates the reduction of the top cover crack widths in the type C tests with respect to the other types of specimens. The maximum delamination crack width for the type C specimen is also shown, in good agreement with the test results.

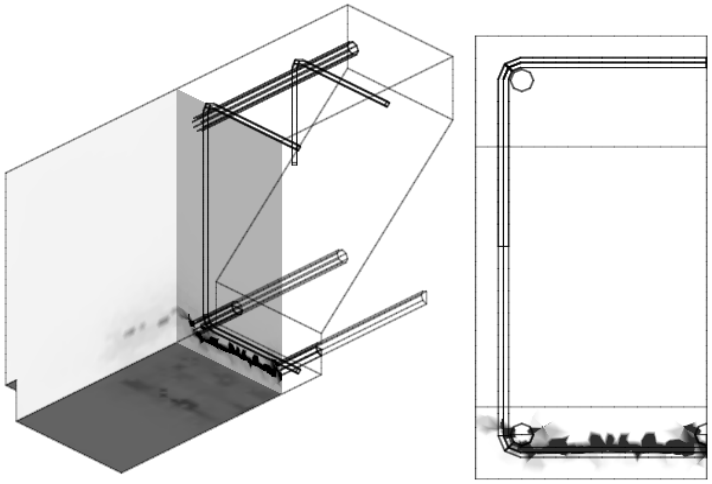

Fig.11 Numerical delamination crack pattern – Type C specimen.

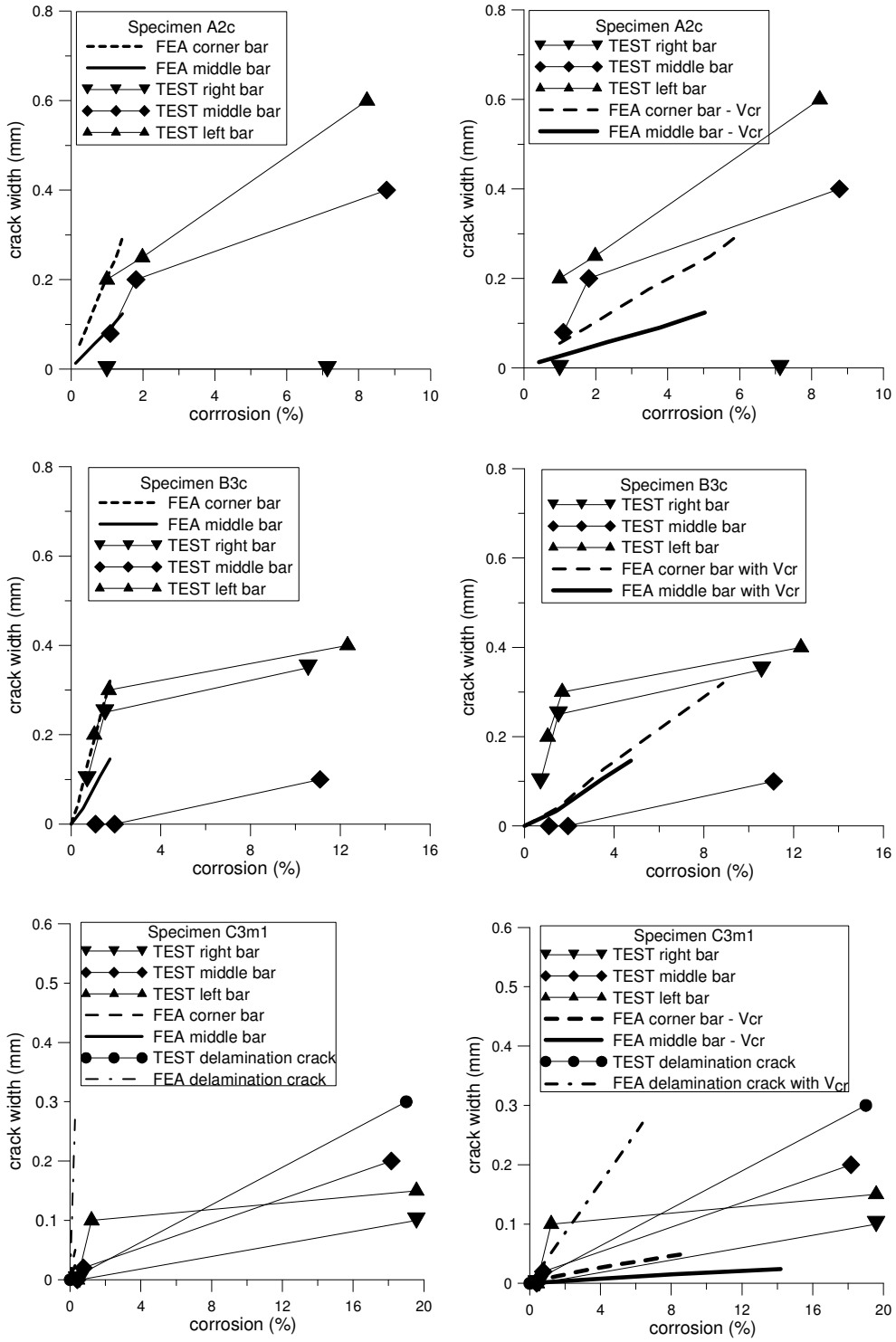

Fig.12 Cracks vs corrosion level: FEA results vs test results up to Level 2 (Type A) and Level 3 (Type B and C).

The maximum amount of corrosion penetration was rather low in the numerical analyses compared with what was observed in the experiments (Fig.12, FEA results in the legend). The model simulates the volume of oxides accumulating around the bar (Equation 4), that is the input of the analysis. As shown by Val et al. (2009), initially this provides a reasonable estimate

of the total volume of oxides and hence of the corrosion level. At this stage a part of the oxides entering the pores of the concrete can be considered too (Liu and Weyers, 1998). When a considerable volume of oxides flows into the cracks, the level of corrosion reached is underestimated, if only the rust accumulated around the bar is considered. In the FEA results the volumetric expansion coefficient was set equal to 2. A higher value of υ_{rs} would cause higher expansion for a given penetration p: the maximum crack width reached in the analyses would correspond to even lower corrosion levels.

To improve the modelling there is the possibility of evaluating *a posteriori* the volume V_{cr} occupied by the cracks in the FE model, using the numerical average crack widths, the length of the cracks and their depth. All the cracks around the bar are taken into consideration. A simplifying assumption is made that the cracks are totally filled by the oxides starting from the first opening.

The crack width to corrosion relation, adding a posteriori the contribution of the volume of the cracks in the calculation of the corrosion level is shown in Fig.12 (FEA with V_{cr} in the legend). The crack volume for each bar, divided by υ_{rs}, accounts for several percentual points of corrosion. A better approximation of the test results is obtained. The low initial inclination of the diagrams, compared to the tests, indicates that differently from what assumed here, rust flow gradually in the cracks. The maximum experimental values of corrosion level are not reached, meaning that a significant quantity of oxides flowed out of the cracks, as was observed experimentally.

To develop the research presented in this paper a model was formulated coupling the cracking and the oxide flow. The volume flow of rust depends on the crack width and also on the splitting stress around the bar. The model is described in Zandi Hanjari et al. (2011-c).

CONCLUSIONS

An experimental program for the mechanical effects of corrosion in reinforced concrete was carried out, investigating high corrosion levels, cover cracking and delamination, and corrosion of the stirrups. An artificial corrosion process with reasonable current density was used. The test results of the corrosion process with the concrete cracking are shown and the numerical simulation, using a 3D finite element model, are presented in this paper. The comparison with existing models for the relation of crack width to corrosion penetration is carried out.

In a first phase of the tests, reaching approximately 1% corrosion, longitudinal cracks opened parallel to the main reinforcement, propagating in the direction of the lower cover. A second phase studied the conditions encountered in highly corroded structures. Even if the complete delamination of the cover did not occur in the tests, a partial propagation of the phenomenon was observed. High corrosion levels are needed to reach the delamination of the cover; using a slow rate of corrosion; this means planning tests with a duration longer than one year of artificial corrosion.

A recent proposal in the literature for a rate of loading correction factor has been used (Mullard and Stewart, 2011), relating the cracking in artificially accelerated corrosion tests to that caused by natural corrosion. By this method the results shown in this paper agree closely to crack measurements in the literature (Vidal et al., 2004) on beams corroding for 14 and 17 years in conditions close to the natural ones, with both main bars and transverse reinforcement

corroding. The same rate of loading correction factor has been applied also to the results shown in the paper for corrosion cracks in specimens without stirrups. The results are close to those of a relation proposed by Mullard and Stewart (2011) for natural corrosion penetration and crack width.

The transverse reinforcement, either corroding or not, reduces the width of cracks caused by corrosion of the main bars. This study shows that stirrup corrosion causes damage quite different from that occurring when stirrups are not corroded; this is useful in linking the knowledge gained in laboratory tests to the damage observed in real structures. Compared to the case when only the main bars corrode, causing mainly longitudinal cracking, with corroded stirrups the damage becomes more severe and diffuse. For a given level of corrosion of the main bars, the damage in a real structure with corroding stirrups is greater than is shown by tests without corroding stirrups.

A numerical 3D FE model was set up to simulate the tests. The results correspond to the experimental observations, with a close reproduction of the crack patterns, and provide an interpretation of the results. A better approximation of the relation between the level of corrosion and the crack widths, using a 3D FE analysis, requires the modelling of the flow of rust into the cracks.

ACKNOWLEDGEMENTS

The technical support for the specimen preparation and casting by Ing. Stefano Vacis and Geom. Giorgio Ghia – AVstrutture is gratefully acknowledged.

REFERENCES

Alonso, C., Andrade, C., Rodriguez, J., Diez, J.M. (1998) "Factors controlling cracking of concrete affected by reinforcement corrosion." *Materials and Structures/Matériaux et Constructions,* V.31, August-September, 435-441

Auyeung, Y., Balaguru, P., Chung, L. (2000) "Bond behavior of corroded reinforcement bars" *ACI Materials Journal,* V.97, No.2, March-April, 214-221.

Berra, M., Castellani, A., Coronelli, D., Zanni, S., Zhang, G. (2003) "Steel-Concrete bond deterioration due to corrosion: FE analysis for different confinement levels." *Magazine of Concrete Research*, 55(3), 237-247.

Bhargava, K., Ghosh, A. K., Mori, Y., Ramanujam, S. (2006) "Model for cover cracking due to rebar corrosion in RC structures." Eng. Struct., 28(8), 1093-1109.

CEB (1998) ''Strategies for testing and assessment of concrete structures.'' Comité Euro-International du Beton *Bulletin 243*, CEB-FIB, Lausanne (CH), Switzerland, 184.

Clark, L.A., Saifullah, M. (1993) "Effect of corrosion on reinforcement bond strength." *Proc. 5th Int. Conf. Structural Faults and Repair*, V.3, Forde, M., Editor, Engineering Technical Press, Edinburgh, 113–119.

Coronelli, D., Gambarova, P. (2004). "Structural assessment of corroded reinforced concrete beams: Modeling guidelines", *ASCE J. Struct. Eng.*, 130(8), 1214-1224.

Diana (2009) "DIANA Finite Element Analysis, User's Manual - Release 9.1", *TNO Building and Construction Research*, Delft, Netherlands.

Fib (2000) "Bond in reinforced concrete." State of the art Report, *fib* Bulletin n.10, 434 pp.

Grassl, P. , Rempling, R. (2007) "Influence of volumetric–deviatoric coupling on crack prediction in concrete fracture tests." Eng. Fract. Mech. 74, 1683–1693.

Higgins, C. and Farrow ,W.C. III (2006), "Tests of Reinforced Concrete Beams with Corrosion-Damaged Stirrups", *ACI Structural Journal*, V. 103, No. 1, January-February 2006, pp.133-141.

Hordijk, D. A. (1991) "Local Approach to Fatigue of Concrete." Doctoral thesis, Delft University of Technology, Delft, Netherlands.

ISO (2009) "ISO 8407. Corrosion of metals and alloys - Removal of corrosion products from corrosion test specimens", *International Organisation for Standardisation*.

Liu, Y. , Weyers, R. E. (1998) "Modeling the time-to-corrosion cracking in chloride contaminated reinforced concrete structures." ACI Mater. J., 95(6), 675-681.

Lundgren, K. (2005a) "Bond between ribbed bars and concrete. Part 1: Modified model." *Magazine of Concrete Research*, Vol. 57, No. 7, pp. 371–382.

Lundgren, K. (2005b) "Bond between ribbed bars and concrete. Part 2: The effect of corrosion." *Magazine of Concrete Research*, Vol. 57, No. 7, pp. 383–395.

Lundgren, K. , S. Roman, A. S., Schlune, H., Hanjari, K. Z. , Kettil, P. (2007) "Effects on bond of reinforcement corrosion." Int. RILEM workshop on *Integral Service Life Modeling of Concrete Structures*, 5-6 November, Guimaraes, Portugal, RILEM Publications S.A.R.L., 231-238.

Molina, F.J., Alonso, C., Andrade, C. (1993) "Cover Cracking as a Function of Rebar Corrosion. 2. Numerical- Model." *Materials and Structures*, 26 (163), 532-548.

Mullard, J.A., Stewart, M.G. (2011), "Corrosion-Induced Cover Cracking: New Test Data and Predictive Models" *ACI Str. Journal* 108(1), 71-79.

Sæther, I. (2009) "Bond deterioration of corroded steel bars in concrete." *Structure and Infrastructure Engineering*, 7(6), 415-429.

Thorenfeldt, E. , Tomaszewicz, A. , Jensen, J.J. (1987) "Mechanical properties of high-strength concrete and applications in design." Conference on *Utilization of High-Strength Concrete*, Stavanger, Norway.

Val, D.V., Chernin, L., Stewart, M.G. (2009). "Experimental and Numerical Investigation of Corrosion-Induced Cover Cracking in Reinforced Concrete Structures" *ASCE J. Struct. Eng.*, 135(4), 376-385.

Vidal, T., Castel, A. , François, R. (2004) “Analyzing crack width to predict corrosion in reinforced concrete.” *Cement and Concrete Research*, 34, 165–174.

Yuan, Y., Ji, Y., Shah, S.P. (2007) “Comparison of Two Accelerated Corrosion Techniques for Concrete Structures.” *ACI Str. J.*, 104(3), 344-347.

Zandi Hanjari, K. , Kettil, P., Lundgren, K. (2011-a) “Analysis of the mechanical behavior of corroded reinforced concrete structures”, A*CI Structural Journal*, 108(5), 532-541.

Zandi Hanjari, K., Coronelli, D., Lundgren, K. (2011-b) “Bond capacity of severely corroded bars with corroded stirrups”, *Magazine of Concrete Research*, 63(12), 953-968.

Zandi Hanjari, K., Lundgren,K., Plos M., Coronelli D. (2011-c) “Three-dimensional modelling of structural effects of corroding steel reinforcement in concrete”, *Structure and Infrastructure Engineering*, Taylor and Francis Ed, DOI:10.1080/15732479.2011.607830.